J. Phys. Chem. A **2001,** *105,* 10899−10905

Studies on 6,6′-Disubstitution Effects of the dpq in $[Ru(bpy)_2(dpq)]^{2+}$ with DFT Method

Kangcheng Zheng,*,† Juping Wang,† Wenlie Peng,‡ Xuewen Liu,† and Fengcun Yun†

School of Chemistry and Chemical Engineering, and School of Life Sciences, Zhongshan University,
Guangzhou 510275, P. R. China

Received: July 11, 2001; In Final Form: September 7, 2001

Theoretical studies on 6,6′-disubstitution effects of the dpq in $[Ru(bpy)_2(dpq)]^{2+}$ are carried out by using DFT method at the B3LYP/LanL2DZ level. The substituent effects caused by the electron-pushing group (OH) and the electron-withdrawing group (F) on the electronic structures and the related properties, e.g., the energies and the components of some frontier molecular orbitals, the spectral properties, and the net charge populations of some main atoms of the complexes, etc., have been investigated. The computational results show that the substituents have some interesting effects on the electronic structures and related properties of the complexes. First, on the basis of the analysis of the frontier molecular orbitals, the substituents influence the first excited-state properties of the substitutive derivates. The electron-withdrawing group (F) can activate the main ligand and passivate the co-ligands in the first excited state of $[Ru(bpy)_2(2F\text{-}dpq)]^{2+}$, whereas the electron-pushing group (OH) does not have this effect in this system. Second, the ground band wavelength of electronic spectra of each of complexes $[Ru(bpy)_2(2R\text{-}dpq)]^{2+}$ (R = OH, H, or F) is shorter slightly than that of well-known complex $Ru(bpy)_3^{2+}$. The substitution of electron-pushing group (OH) or electron-withdrawing group (F) on 6,6′ sites of dpq in $[Ru(bpy)_2(dpq)]^{2+}$ can cause a slight red shift in the ground band of the complex. Third, some interesting characteristics of atomic net charge populations on the main ligands of the three complexes occur, and they can be simply and satisfactorily interpreted applying the schematic map expressed by several series of arrowheads, based on the law of polarity alternation and the idea of polarity interference. The above theoretical results should be important to further inquiry into the interaction mechanism of the complexes with DNA active units from both the molecular orbital interactions and the atomic charge interactions.

Introduction

Octahedral Ru(II) polypyridyl complexes have aroused more and more interest from researchers because of their extensive applications to the fields of photochemistry, photophysics, photocatalysis, electrochemistry, biochemistry, and so on, especially because of their important applications to DNA-binding, electrochemical luminescence, and solar energy battery material.[1−5] Recently, a great deal of this kind of complexes and their substitution derivates have been synthesized. To investigate their interaction mechanism with DNA, many new substituted derivates on the main ligands of Ru(II) polypyridyl complexes have been designed and synthesized.[6−11] Three types of binding modes (i.e., electrostatic binding mode, groove binding mode, and intercalative binding mode) have been proposed for explaining the interaction mechanism between the complexes and DNA.[12−16] Despite much published material, they still mostly remain on experimental researches on this field, and the mechanisms of chemo- or bioreactions of these complexes with DNA are still a controversial issue.[17−23] It may be a difficult subject to essentially understand the interaction mechanism of the complexes with DNA unless we can discuss them at a level of the molecular electronic structure; that is to say, unless we can analyze them from the interaction between molecular orbitals, especially some frontier molecular orbitals, or the interaction between atomic charges because such two kinds of interactions are closely related to the three above-mentioned types of binding modes of the complexes to DNA. It is undoubtedly quite a difficult theoretical task. But as a preliminary approach, it is absolutely possible and very significant to investigate the electronic structures and the related properties of Ru(II) polypyridyl complexes. In particular, the binding between the complex and DNA generally happens on the main ligand of the complex; therefore, it is very important to theoretically analyze the characteristics of “electron cloud” distributions on the frontier molecular orbitals and the atomic net charge populations of the main ligand of the complexes. The quantum chemical computations can play a role in elucidating the electronic structures and the related properties of the complexes.

With the high-speed development of computer technology and the wide applications of G94/G98 program packages,[24,25] more and more quantum chemical computations on transition metal complexes, in particular, the computations applying density functional theory(DFT), have been reported[26−34] because of their better performance for electron correlation energies and reducing greatly the computation expenses. When quantum chemical computations are applied to transition metal polypyridyl complexes with relatively large size, undoubtedly the computations of energies and spectral properties of those complexes in an absolute meaning have still some errors. We think that the most important thing is to obtain some regularities or trends in the electronic structures and related properties of the similar complexes, which can be used for references in the synthesis of the complexes and the mechanism analysis on the photochemistry, electrochemistry, catalysis chemistry, and biochemistry of the complexes. For this purpose, we have recently reported the theoretical results on the complexes $M(bpy)_3^{2+}$(M = Fe, Ru, Os),[35] $[Ru(4,4'\text{-}2R\text{-}bpy)_3]^{2+}$,[36] $[Ru(bpy)_2(4,4'\text{-}2R\text{-}bpy)]^{2+}$,[37] $[Ru(bpy)_2\ (5,6-2R\text{-}phen)]^{2+}$,[38] $M(bpy)_3^{n+}$(M = Re, Os, Ir; $n = 1, 2, 3$, respectively),[39] and $[Ru(phen)_2\ (5,6-2R\text{-}phen)]^{2+}$,[40] etc., with DFT method.

---

* To whom correspondence should be addressed. Email: ceszkc@zsu.edu.cn.

† School of Chemistry and Chemical Engineering.

‡ School of Life Sciences.

10.1021/jp0126560 CCC: $20.00

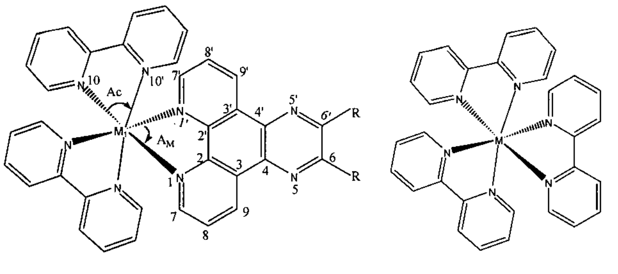

(a) **I**~ **III** (b) **IV**

Figure 1. Computation models of $[Ru(bpy)_2(2R\text{-}dpq)]^{2+}$ (R = OH, H and F; **I**, **II** and **III**, respectively) and $[Ru(bpy)_3]^{2+}$ (**IV**).

In this paper, we report the theoretical results on 6,6′-disubstitution effects of the dpq in $[Ru(bpy)_2(dpq)]^{2+}$ (dpq= dipyrido [3,2-d:2′,3′-f] quinoxaline, bpy = 2,2′-bipyridyl) with the DFT method. The trends in the substituents affecting the electronic structures and the related properties of the complexes, e.g., the energies and the compositions of some frontier molecular orbitals, the spectral properties, and the net charge populations on some main atoms of the complexes, the main bond lengths and bond angles of the complexes, etc., have been investigated.

Computation and Method

Octahedral bidentate complex $[Ru(bpy)_2(dpq)]^{2+}$ forms from Ru(II) with an intercalative ligand dpq called the main ligand and two bpy ligands called the co-ligands and belongs to C_2 symmetry. When two H atoms on 6,6′ sites (in Figure 1) of dpq ligand are replaced by two identical substituents R (R = OH or F), the symmetry does not change. Full geometry optimizations of the three complexes starting at C_2 symmetry are carried out with DFT method at B3LYP/LanL2DZ level. In the computations, the singlet states are taken because of the low electronic spin for the complexes.[1] About 67−69 atoms are involved in every complex. In addition, the computations on complex $Ru(bpy)_3{}^{2+}$ are also carried out for comparisons. All computations of these complexes are performed with G98 quantum chemistry program-package[25] on PentiumIII (933M Hz) computers. To vividly depict the detail of the frontier molecular orbital interactions, the stereographs of HOMO (the highest occupied molecular orbital) and LUMO (the lowest unoccupied molecular orbital) of the complexes are drawn with Molden v3.6 program[41] based on the above computational results.

It is very important to study the trend in atomic net charge distribution of a molecule because of its close relation to active site in electrophilic or nucleophilic reactions and the charge interactions between it and other molecules. The net charge populations of the three complexes are computed using the natural orbital population analysis(NPA)[42,43] in G98 program packages. At the same time, to analyze the net charge population characteristics of complicated systems containing more than one substituent or skeleton heteroatom, schematic maps of electronic effect interference expressed by several series of arrowheads should be drawn on the basis of the law of polarity alternation[44−46] and the idea of polarity interference.[47,48] The former maintains that inductive effects are transmitted in a charge-alternate way like conjugation effects (up to now, inductive effects are still maintained to be transmitted in an unidirectional way in some text books). The electron effects (induction and conjugation) gradually attenuate in transmission path. The latter thinks that for any molecule containing more than two atoms, the polarity of any bond (and then the corresponding charge transfer) depends on not only the primary polarity (i.e, the one caused by only the difference between the electronegativities of the two bound atoms), but also the polarity interference from the electronic effect (i.e, algebraic sum of electronic effects including conjugation and induction). Such a polarity interference on a discussed bond can be expressed as the algebraic sum of primary polarity of a bond and polarity of electronic effects. If the polarity effects and the primary polarity are the same in direction, a constructive polarity interference occurs, making the polarity and intensity of the bond increase, and then the alternation of positive and negative charges on the bond-end atoms will be strengthened; that is to say, the charge transfer increases. On the contrary, if both are opposite in directions, a destructive polarity interference occurs, causing contrary trends in change of bond polarity, bond intensity, and charge alternation. For biatomic molecules, the bond polarity has been well-defined as bond dipole moment for a long time. It is produced by the electron density distribution in covalent bonds due to difference in electronegativity of the bound atoms, so its direction points to more electronegative atom, and its size

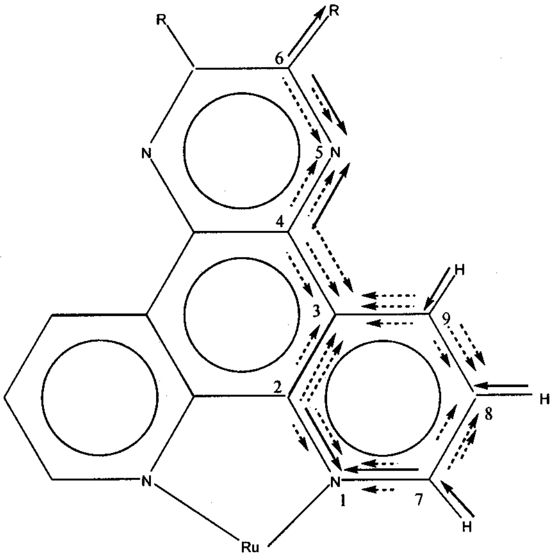

Figure 2. Schematic representation of atomic net charge populations along two important paths from R (R = OH or F) to N1 in complexes **I** and **III**.

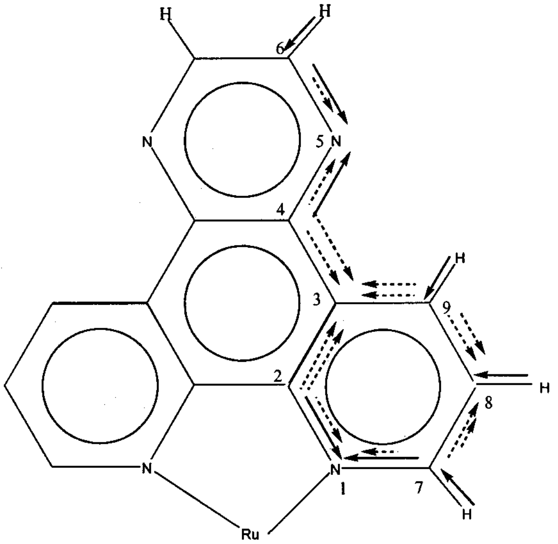

Figure 3. Schematic representation of net charge populations along two important paths from R (R = H) to N1 in complex **II**.

TABLE 1: Computational Results on the Main Bond Lengths (nm) and Bond Angles (deg) of the Complexes

comp.		$Ru-N_m$[a]	$Ru-N_{co}$	A_m[b]	A_{co}	$C-C_m(C-N_m)$[c]	$C-C_{co}(C-N_{co})$
I (R = OH)		0.2110	0.2097	79.2	78.5	0.1398	0.1394
II (R = H)		0.2110	0.2098	79.2	78.4	0.1400	0.1394
III (R = F)		0.2110	0.2099	79.2	78.5	0.1396	0.1394
IV	calc	0.2101	0.2101	78.4	78.4	0.1394	0.1394
($Ru(bpy)_3^{2+}$)	expt	0.2056	0.2056	78.7	78.7	0.1360	0.1360

[a] $Ru-N_m$ expresses coordination bond length between the center ion and the main ligand (dpq), and so on. [b] A_m expresses coordination bond angle between the center ion and the main ligand (dpq), and so on. [c] $C-C_m(C-N_m)$ expresses the mean bond lengths of the main ligand skeleton, and so on.

TABLE 2: Main Atomic Orbital Populations of NHOMO, HOMO, LUMO and NLUMO in $[Ru(bpy)_2(2R\text{-}dpq)]^{2+}$ and $[Ru(bpy)_3]^{2+}$(%)

		Ru			N_m[a]		C_m		H_m	R_m		N_{co}[b]		C_{co}		H_{co}
comp.		s	p	d	s	p	s	p	s	s	p	s	p	s	p	s
I	NH	0.0	0.1	51.2	0.0	2.6	0.0	28.3	0.0	0.0	7.5	0.2	1.3	2.0	6.8	0.0
	H	0.1	0.0	77.9	0.0	1.2	1.5	4.5	0.0	0.0	0.0	0.0	2.4	2.7	9.6	0.0
	L	0.0	0.2	0.8	0.2	2.3	0.3	9.8	0.0	0.0	0.0	0.2	24.2	0.3	61.9	0.0
	NL	0.0	0.0	6.2	0.3	0.3	0.2	0.7	0.0	0.0	0.0	0.4	27.0	0.3	64.8	0.0
II	NH	0.0	0.3	71.5	0.0	0.6	0.0	13.0	0.0	0.0	–	0.2	1.8	2.7	9.8	0.0
	H	0.1	0.0	78.0	0.0	1.2	1.5	4.5	0.0	0.0	–	0.0	2.4	2.6	9.6	0.0
	L	0.0	0.2	0.4	0.2	3.9	0.3	13.6	0.0	0.0	–	0.2	22.6	0.3	58.3	0.0
	NL	0.0	0.0	6.2	0.3	0.3	0.2	0.9	0.0	0.0	–	0.4	27.0	0.3	64.6	0.0
III	NH	0.0	0.3	71.7	0.0	0.5	0.0	12.8	0.0	0.0	0.2	0.2	1.8	2.7	9.8	0.0
	H	0.1	0.0	77.9	0.0	1.1	1.6	4.5	0.0	0.0	0.0	0.0	2.5	2.6	9.6	0.0
	L	0.0	0.2	0.3	0.1	16.6	0.1	42.4	0.0	0.0	0.3	0.3	10.7	0.4	28.8	0.0
	NL	0.0	0.1	5.2	0.2	11.3	0.2	27.8	0.0	0.0	0.3	0.3	16.1	0.2	38.5	0.0

[a] N_m expresses all N atoms in the main ligand. [b] N_{co} expresses all N atoms in the co-ligands (note: two co-ligands).

is directly proportional to the quantity of transferred charges which can be estimated according to the following formula[49]

$$\Delta Q_X = \frac{nX_C - X_X}{X_X + X_C}$$

where ΔQ_X represents transferred charge onto the X atom, X_C and X_X represent the electronegativity of the C atomic orbital and that of the X atomic orbital, respectively, and n represents number of electron in the X orbital ($n = 2$ for a lone pair electrons, $n = 1$ generally for other cases).

Up to now, the bond polarity in polyatomic molecule has not been defined, so we cannot yet derive a general formula for calculating the bond polarity, but this obstacle does not affect our qualitative discussions for its relative properties (i.e., the energies of isomers, the bond-lengths and the charge populations, etc.) in order to obtain the related trends or regularities.

For the above purpose, we first should draw sketches of polarity interference as Figure 2 and Figure 3, where a solid arrowhead toward a more electronegative atom represents primary bond polarity (the total result including induction and conjugation), for example, a solid arrowhead points toward the more electronegative atom N, or O, or F from the C atom, etc. Two series of alternately directional and gradually shortened dotted arrowheads on the right (or top) of every skeleton bond line represent the gradually reduced polarity of electronic effect (total of induction and conjugation) caused by the two skeleton N atoms, and that on the left (or bottom) of every skeleton bond line represents the gradually reduced polarity of the electron effect caused by R (comparing Figures 2 and 3, easy to distinguish the effects caused by R and N atoms). The directions of dotted arrowheads are determined according to the law of polarity alternation. Each arrowhead shows the direction of moving negative charges on a bond. Because the quantity of transferred charges between the two directly adjoining atoms should be larger than that between the two indirectly adjoining atoms, the quantity of transferred charges represented by a solid arrowhead should be larger than that represented by a dotted arrowhead. Therefore, the relative size and sign of net charges on each atom can be explained or predicted according to the lengths, numbers, and directions of solid arrowheads and dotted arrowheads.

Results and Discussion

Substituent Effects on Main Bond Lengths and Bond Angle of the Complexes. The computational results for the main bond lengths and bond angles of the complexes are shown in Table 1.

So far, the reports on crystal structures of above three complexes have still not been found. We cannot directly compare their computational results with experimental values. But the computational results are reliable because they are nearly in agreement with the reported experimental values of analogous complexes. For example, the reported experimental coordination bond lengths Ru–N (bpy), are within 0.199–0.213, 0.202–0.209, 0.204–0.209, and 0.205–0.210 nm for *cis*-$Ru(bpy)_2(py)_2(BF_4)_2$,[50] $Ru(bpy)_2$ $(5\text{-}CH_3\text{-}phen)(ClO_4)_2$,[8] $Ru(bpy)_2(phen)(ClO_4)_2 \cdot H_2O$,[8] and $Ru(bpy)_2$ $[C_6H_4(NH)_2](PF_6)_2$,[51] respectively, and their coordination bond angles N–Ru–N(bpy) are 77–85°, 76.4–77.9°, 78.6–78.8°, and 78.2–78.3°, respectively.The computed coordination bond lengths (see Table 1) are all within the above range, and the bond-angles are also within or near to the above range (see Table 1). In particular, comparing the computational results with the main experimental data of well-known complex $Ru(bpy)_3^{2+}$(**IV**)[52] in Table 1, we can find that the computational coordination bond lengths (Ru–N) and the mean bond lengths of C–C(C–N) are larger than the corresponding experimental values only by 1–2%, the computational coordination bond angles (A) are also less than the experimental values only by ~1%, and the mean bond-lengths C–C (N) of the ligand skeletons approach the standard bond-length (0.140 nm). The errors can be considered to come mainly from two factors: One is that theoretical computations do not consider the effects of chemical environment (as a free molecule), and the other one is that the calculation method and basis set are still approximate in some extent. However, the computational results are significant for discussion of the properties of large systems. Therefore, on the basis of the geometries of the complexes obtained from the full optimization computations, we can further carry out the study on the trends in the substituent effects on the electronic structures and the related properties of the complexes.

From Table 1, we can see that the substituent effects on main bond lengths and bond angles of the complexes are trivial. Even now, the electron-pushing group (OH) and the electron-withdrawing group (F) both can slightly shorten the average bond length of C–C (and C–N) of the main ligand and the electron-withdrawing group (F) can shorten it more, but they both nearly have no effect on average bond lengths of C–C (and C–N) in the co-ligands because they are remote from the co-ligands. It shows that when two H atoms on 6,6′ sites (in

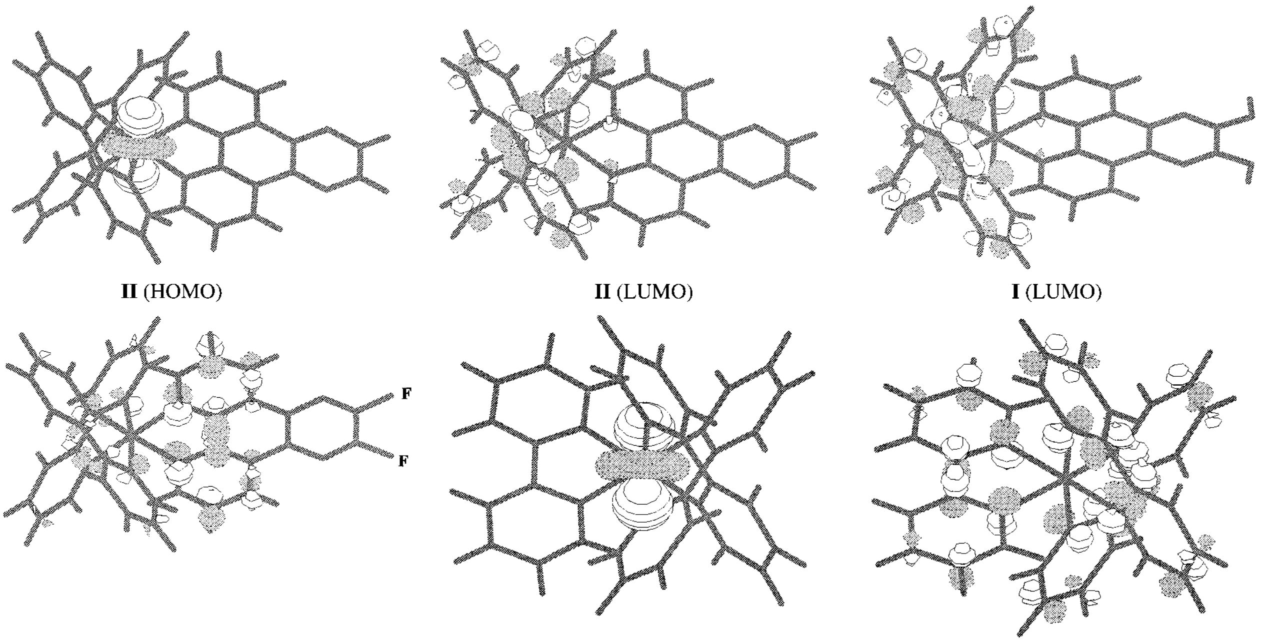

II (HOMO) **II** (LUMO) **I** (LUMO)

III (LUMO) **IV** (HOMO) **IV** (LUMO)

Figure 4. Stereographs of HOMO and LUMO of complexes (**I**−**IV**) (stereographs of HOMO of **I** and **III** are omitted because of being similar to those of **II** and **IV**).

Figure 1) of ligand dpq are replaced by two identical substituents R (R = OH or F), the aromatic ring skeleton of the main ligand will become slightly more stable. In addition, compared **I**, **II**, and **III** with $Ru(bpy)_3^{2+}$ (**IV**), we can also find that when a ligand (bpy) is subsitituted by dpq or 2R-dpq, the bond length $Ru-N_m$ will be increased, and the bond $Ru-N_{co}$ will be slightly shortened.

Substituent Effects on Frontier Molecular Orbital Components. To study the substituent effects on spectral properties and excited states of complexes, some frontier molecular orbital compositions (or atomic orbital populations) have been analyzed. The atomic orbital populations for a varied type of atomic orbitals (e.g., s, p, d orbitals) in specific molecular orbitals, e.g., HOMO, LUMO, NHOMO (the next HOMO), and NLUMO (the next LUMO), are expressed as the atomic orbital coefficient square sum in the type of atomic orbitals and corrected by normalizing the specific molecular orbital. The results are shown in Table 2. The stereographs of the four orbitals are further shown in Figure 4.

Some population characteristics of the frontier molecular orbitals of $[Ru(bpy)_2(2R\text{-}dpq)]^{2+}$ will be seen from Table 2 and Figure 4 as follows:

(1) The components of HOMO and NHOMO of the three complexes (**I**−**III**) come mainly from d orbitals of the center metal ions, i.e., they may be characterized by d orbitals of the metal ions, and the components of LUMO and NLUMO come mainly from p orbitals of C and N atoms in ligands, i.e., they may be characterized by p orbitals of the ligands, so on the basis of the analysis of frontier molecular orbitals, the electronic ground bands and the next ground bands of complexes **I**−**III** are all assigned theoretically to singlet metal-to-ligand charge-transfer transitions (^{1}MLCT) similar to those of $Ru(bpy)_3^{2+}$ (**IV**).[1] However, the energy difference between the ground and the next ground is too small to be distinguished, and then usually only a broad ^{1}MLCT band appears for them in electronic absorption spectra.[1]

(2) It is very interesting that the substituents have obvious effects on the components of the LUMO. Although the electronic ground bands and the next ground bands of the three complexes (**I**−**III**) are all assigned to singlet metal-to-ligand charge-transfer transitions (^{1}MLCT), the special spectral properties are different. When an electron transfers from HOMO to LUMO, for complex **I** and **II**, the "electron cloud" in the LUMO (original) is mainly populated on the p orbitals of C and N in the two co-ligands, whereas for complex **III**, the "electron cloud" in the LUMO (original) is mainly populated on the p orbitals of C and N in the main ligands. Therefore, we can come to an important trend: The substituent of the electron-withdrawing group (F) can activate the main ligand and passivate the co-ligand in the first excited state, whereas the electron-pushing group (OH) has no this effect.

Undoubtedly, considering electron transfer from HOMO to LUMO as a transition from the ground state to the first excited state is only a well-approximation, but according to the frontier molecular orbital theory,[53] HOMO and LUMO play an predominant role in general chemical reactions and related properties of compounds; such a well-approximation is very advantageous to discuss some relative regularities or trends. In regard to the excited states, the further computations need density-functional theory for excited states, in which a Kohn−Sham formalism of excited states with the density-functional theory (DFT) is presented, and the differences of Kohn−Sham eigenvalues are also shown to be well-defined approximations for excitation energies.[54] So it should be significative to discuss some trends from the frontier molecular orbitals and their energies (i.e., eigenvalues) based on DFT.

Substituent Effects on Frontier Molecular Orbital Energies and Spectral Properties of the Complexes. Occupied frontier molecular orbital energies are related to photoelectron spectra, and the intervals of frontier molecular orbital energies are related to UV spectra. Some frontier molecular orbital energies and the corresponding energy intervals are listed in Table 3. For a simple comparison, the schematic map of the energy levels of the NHOMO, HOMO, LUMO, and NLUMO and the related electronic energy transitions are shown in Figure 5.

From Table 3 and Figure 5, we can find two interesting charateristics of the substituent effects on frontier molecular orbital energies and spectral properties.

TABLE 3: Some Frontier Molecular Orbital Energies of $[Ru(bpy)_2(dpq)]^{2+}$ and Its Substituted Derivates (ϵ_i/au)

comp.	Occ	Occ	Occ	Occ	NHOMO	HOMO	LUMO	NLUMO	Vir	$\Delta\epsilon_{L-H}$
I	1a −0.4501	2a −0.4482	1b −0.4164	3a −0.4091	2b −0.4053	4a −0.4028	3b −0.2787	5a −0.2755	4b −0.2716	0.1241
II	1a −0.4546	1b −0.4488	2a −0.4271	3a −0.4110	2b −0.4096	4a −0.4047	3b −0.2803	4b −0.2770	5a −0.2747	0.1244
III	1a −0.4623	1b −0.4614	2b −0.4561	2a −0.4179	3b −0.4168	3a −0.4117	4b −0.2873	5b −0.2833	4a −0.2826	0.1243
IV	1a1 −0.4599	1e −0.4579	1e′ −0.4579	2e −0.4134	2e′ −0.4134	2a1 −0.4071	1a2 −0.2832	3e −0.2791	3e′ −0.2791	0.1239

TABLE 4: Atomic Net Charge Populations of the Main Ligand of Complexes I−III (Unit: |e|)

(a) Along Path R−C6−N5−C4−C3−C2−N1

comp.	R	C6	N5	C4	C3	C2	N1	Ru
I (R = OH)	−0.1385	0.5634	−0.5391	0.1761	−0.0558	0.2010	−0.4747	0.6274
II (R = H)	0.2422	0.0659	−0.4559	0.1858	−0.0568	0.2049	−0.4754	0.6270
III (R = F)	−0.3096	0.6100	−0.4681	0.1853	−0.0609	0.2071	−0.4735	0.6273

(b) Along Path R−C6−N5−C4−C3−C9−C8−C7−N1

comp.	R	C6	N5	C4	C3	C9	C8	C7	N1	Ru
I (R = OH)	−0.1385	0.5634	−0.5391	0.1761	−0.0558	−0.1213	−0.2161	0.0926	−0.4747	0.6274
II (R = H)	0.2422	0.0659	−0.4559	0.1858	−0.0568	−0.1156	−0.2137	0.0954	−0.4754	0.6270
III (R = F)	−0.3096	0.6100	−0.4681	0.1853	−0.0609	−0.1157	−0.2102	0.0995	−0.4735	0.6273

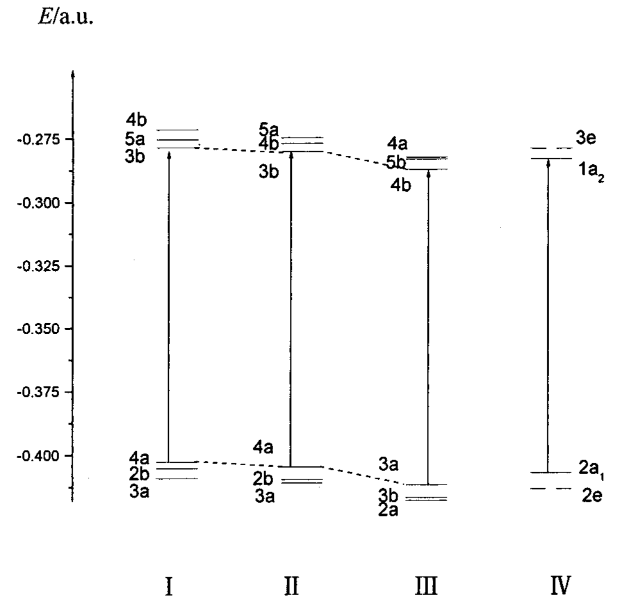

Figure 5. Schematic map of energies of some frontier MO and the related electronic energy transitions of $[Ru(bpy)_2(2R\text{-}dpq)]^{2+}$ (**I−III**) and $[Ru(bpy)_3]^{2+}$ (**IV**).

(1) For complexes **I−III**, with an increase in electron-withdrawing ability of R, the corresponding frontier molecular orbital energies are all decreased. We can understand it as follows: The three complexes are so large conjugated systems. Their some frontier molecular orbitals, in particular, HOMO and LUMO, are mainly π-type molecular orbitals, and they are very sensitive to substituent properties. With an increase in electron-withdrawing ability of the substituent, its Coulombic attraction for frontier molecular orbitals is strengthened, so there is the above trend.

(2) The energy interval $\Delta\epsilon_{L-H}$ between LUMO and HOMO of complex **II** is the greatest in complexes **I−III**. In addition, $\Delta\epsilon_{L-H}$ for each of three complexes **I−III** is greater than that for complex **IV**. As known, since the intervals of frontier molecular orbital energies are related to UV spectra, we can deduce that: First, the wavelength of electronic ground band for each of complexes **I−III** will be shorter slightly than that of complex **IV**. Such a prediction bas been proved by part of experiments. For example, the experimental wavelength of the ground band of $[Ru(bpy)_2(dpq)]^{2+}$ (**II**) is 449 nm,[55] and that of $[Ru(bpy)_3]^{2+}$ (**IV**) is 452 nm[1,56] though those of complexes **I** and **III** are not found. Second, the electron-pushing group (OH) or electron- withdrawing group (F) will cause a slight red shift in the ground band of the complex when the two H atoms on 6,6′ sites of dpq in $[Ru(bpy)_2(dpq)]^{2+}$ are replaced by two identical substituents R (OH or F).

Substituent Effects on the Atomic Net Charge Populations of Complexes. According to the natural orbital population analysis (NPA), the net charge populations of some main atoms in the $[Ru(bpy)_2(2R\text{-}dpq)]^{2+}$ (R = OH, H, F) are shown in Table 4.

From Table 4, the following characteristics of the net charge populations can be seen:

(1) Along path (a) R → C6 → N5 → C4 → C3 → C2 → N1, the net atomic negative charges clearly alternate with the net atomic positive charges for **I** (R = OH) and **II** (R = F).

(2) The charge distribution does not entirely alternate along path a for **II** (R = H) because H charges positively instead of negatively.

(3)Along path (b) R → C6 → N5 → C4 → C3 → C9 → C8 → C7 → N1, the atomic net charge distribution basically alternates for **I** and **III** (except atom C9 charging negatively instead of positively).

(4) The most negative charges are populated on N1 or N5, and the next are populated on C8 among all atoms of aromatic ring skeletons for complexes **I−III**.

(5) The substituent R (OH or F) can greatly influence charge populations on its near neighboring atoms, but less influences those on the atoms far from it (i.e., near N1).

The above-mentioned characteristics of atomic charge populations in heterocyclic system cannot be explained with the traditional schematic map expressed by a single series of winding arrowheads generally used in textbook of organic chemistry,[57] which can explain the net charge populations on some uni-substituted benzenes because of a fully equal chemical environment of every C atom in benzene, but they may be simply and satisfactorily interpreted applying above-mentioned schematic maps expressed by several series arrowheads.

Comparing Table 4 with Figures 2 and 3, the above characteristics of atomic charge populations can be well explained as follows: Character 1 is because of the constructive polarity interference (the sum of transferred charges with the same sign on every atom) of electronic effects from N1, N5, and R (R = OH or F) each other. It can be easily seen that along path a, for complexes **I** and **III** (R = OH, F), R, N5, C3, and N1 all carrying net negative charges are just the ones the arrowheads advance toward, whereas the atoms C6, C4, and C2 carrying net positive charges are the ones the arrowheads depart from as Figure 2. Character 2 is because of transfer of negative charges from H to C6 (solid arrowhead from H to C6). Character 3 is because of transfer of negative charges from H to C9 (solid arrowhead from H to C9); it makes C9 atom carry negative charges instead of positive charges. Character 4 is because of two solid arrowheads and four dotted arrowheads toward N5 and N1 and one solid arrowhead and six dotted arrowheads toward C8 for complexes **I** and **III**, and two solid arrowheads and two dotted arrowheads toward N5 and N1, and one solid arrowhead and four dotted arrowheads toward C8 for complex **II**. Character 5 is because of the rapid decay of the electronic effect of R (especially the inductive effect in the total electronic effect) with an increase in distance between R and the discussed atoms.

Summary

The theoretical studies on 6,6′-disubstitution effects of the dpq in $[Ru(bpy)_2(dpq)]^{2+}$ using DFT method at the B3LYP/LanL2DZ level show that substituents have some interesting effects on the electronic structures and related properties of the complexes. First, on the basis of the analysis of the frontier molecular orbitals, the substituents influence the first excited-state properties of the substitutive derivates. The electron-withdrawing group (F) can activate the main ligand and passivate the co-ligands in the first excited states of $[Ru(bpy)_2(2F\text{-}dpq)]^{2+}$, whereas the electron-pushing group (OH) does not have this effect in this system. Second, the ground band wavelength of electronic spectra of each of complexes $[Ru(bpy)_2(2R\text{-}dpq)]^{2+}$ (R = OH, H, or F) is shorter slightly than that of well-known complex $Ru(bpy)_3{}^{2+}$. The substitution of electron-pushing group (OH) or electron-withdrawing group (F) on 6,6′ sites of dpq in $[Ru(bpy)_2(dpq)]^{2+}$ can cause a slight red shift in the ground band of the complex. Third, there are some apparent characteristics of atomic net charge populations on the main ligands of the three complexes. The most negative charges are populated on N1 or N5, and the next most negative charges are populated on C8 in all atoms of the aromatic ring skeleton. The complicated charge population characteristics may be simply and satisfactorily interpreted applying the schematic map expressed by several series of arrowheads, based on the law of polarity alternation and the idea of polarity interference. The above theoretical study results should be important to further inquire into the interaction mechanism of the complexes with DNA active units from both the molecular orbital interactions and the atomic charge interactions.

Acknowledgment. The financial support of National Natural Science Foundation of the People's Republic of China is gratefully acknowledged.

Note Added after ASAP Posting. This paper originally appeared on the Web on 11/03/01 with different data in Table 1. The revised version was posted on 11/6/01.

References and Notes

(1) Juris, A.; Balzani, V.; Barigelletti, F.; Campagna, S.; Belser, P.; Zelewsky, A. V. *Coord. Chem. Rev.* **1988**, *84*, 85.
(2) Kalyanasundaram, K. *Coord. Chem. Rev.* **1982**, *46*, 159.
(3) Balzani, V.; Juris, A.; Venturi, M.; Campagna, S.; Serroni, S. *Chem. Rev.* **1996**, *96*, 759.
(4) MacDonnell, F. M.; Kim, M. J.; Bodige, S. *Coord. Chem. Rev.* **1999**, *185*−*186*, 535.
(5) Krausz, E.; Risen, H.*Coord. Chem. Rev.* **1997**, *159*, 9.
(6) Zhen, Q. X.; Ye, B. H.; Liu, J. G.; Zhang, Q. L.; Ji, L. N.; Wang, L. *Inorg. Chim. Acta* **2000**, *303*, 141.
(7) Ye, B. H.; Ji, L. N.; Xue, F.; Mak, T. C. W. *Transition Met. Chem.* **1999**, *24*, 8.
(8) Ye, B. H.; Chen, X. M.; Zeng, T. X.; Ji, L. N. *Inorg. Chim. Acta* **1995**, *240*, 5.
(9) Ruminski, R. R.; Deere, P. T.; Olive, M.; Serveiss, D. *Inorg. Chim Acta* **1998**, *281*, 1.
(10) Bhuiyan, A. A.; Kincaid, J. R. *Inorg. Chem.* **1999**, *38*, 4759.
(11) Bodige, S.; MacDonnell, F. M. *Tetrahedron Lett.* **1997**, *38*, 8159.
(12) Xiong, Y.; Ji, L. N. *Coord. Chem. Rev.* **1999**, *185*−*186*, 711.
(13) Marincola, F. C.; Casu, M.; Saba, G.; Lai, A.; Lincoln, P.; Norden, B. *Chem. Phys.* **1998**, *236*, 301.
(14) Lincoln, P.; Norden, B. *J. Phys. Chem. B* **1998**, *102*, 9583.
(15) Coggan, D. Z. M.; Haworth, I. S.; Bates, P. J.; Robinson, A.; Rodger, A. *Inorg. Chem.* **1999**, *38*, 4486.
(16) Choi, S. D.; Kim, M. S.; Kim, S. K.; Lincoln, P.; Tuite, E.; Nordén, B. *Biochem.* **1997**, *36*, 214.
(17) Barton, J. K.; Danishefsky, A. T.; Goldberg, J. M. *J. Am. Chem. Soc.* **1984**, *106*, 2172.
(18) Barton, J. K.; Goldberg, J. M.; Kumar, C. V.; Turro, N. J. *J. Am. Chem. Soc.* **1986**, *108*, 2081.
(19) Hiort, C.; Nordén, B.; Rodger, A. *J. Am. Chem. Soc.* **1990**, *112*, 1971.
(20) Haworth, I. S.; Elcock, A. H.; Freeman, J.; Rodger, A.; Richards, W. G. *J. Biomol. Struct. Dyn.* **1991**, *9*, 23.
(21) Erikson, M.; Leijon, M.; Hiort, C.; Nordén, B.; Grasund, A. *J. Am. Chem. Soc.* **1992**, *114*, 4933.
(22) Satyanarayana, S.; Dabrowiak, J. C.; Chaires, J. B. *Biochemistry* **1992**, *31*, 9319.
(23) Satyanarayana, S.; Dabrowiak, J. C.; Chaires, J. B. *Biochemistry* **1993**, *32*, 2573.
(24) Frisch, M. J.; Trucks, G. W.; Schlegel, H. B.; Gill, P. M. W.; Johnson, B. G.; Robb, M. A.; Cheeseman, J. R.; Keith, T.; Petersson, G. A.; Montgomery, J. A.; Raghavachari, K.; Al-Laham, M. A.; Zakrzewski, V. G.; Ortiz, J. V.; Foresman, J. B.; Cioslowski, J.; Stefanov, B. B.; Nanayakkara, A.; Challacombe, M.; Peng, C. Y.; Ayala, P. Y.; Chen, W.; Wong, M. W.; Andres, J. L.; Replogle, E. S.; Gomperts, R.; Martin, R. L.; Fox, D. J.; Binkley, J. S.; Defrees, D. J.; Baker, J.; Stewart, J. P.; Head-Gordon, M.; Gonzalez, C.; Pople, J. A. *Gaussian 94*, revision D.3; Gaussian, Inc.: Pittsburgh, PA, 1995.
(25) Frisch, M. J.; Trucks, G. W.; Schlegel, H. B.; Scuseria, G. E.; Robb, M. A.; Cheeseman, J. R.; Zakrzewski, V. G.; Montgomery, J. A., Jr.; Stratmann, R. E.; Burant, J. C.; Dapprich, S.; Millam, J. M.; Daniels, A. D.; Kudin, K. N.; Strain, M. C.; Farkas, O.; Tomasi, J.; Barone, V.; Cossi, M.; Cammi, R.; Mennucci, B.; Pomelli, C.; Adamo, C.; Clifford, S.; Ochterski, J.; Petersson, G. A.; Ayala, P. Y.; Cui, Q.; Morokuma, K.; Malick, D. K.; Rabuck, A. D.; Raghavachari, K.; Foresman, J. B.; Cioslowski, J.; Ortiz, J. V.; Stefanov, B. B.; Liu, G.; Liashenko, A.; Piskorz, P.; Komaromi, I.; Gomperts, R.; Martin, R. L.; Fox, D. J.; Keith, T.; Al-Laham, M. A.; Peng, C. Y.; Nanayakkara, A.; Gonzalez, C.; Challacombe, M.; Gill, P. M. W.; Johnson, B. G.; Chen, W.; Wong, M. W.; Andres, J. L.; Head-Gordon, M.; Replogle, E. S.; Pople, J. A. *Gaussian 98*, revision A.9; Gaussian, Inc.: Pittsburgh, PA, 1998.
(26) Ziegler, M.; Zelewsky, A. V. *Coord. Chem. Rev.* **1998**, *177*, 257.
(27) Damrauer, N. H.; Weldon, B. T.; McCusker, J. K. *J. Phys. Chem. A* **1998**, *102*, 3382.
(28) Petersson, G. A.; Malick, D. K.; Wilson, W. G. *J. Chem. Phys.* **1998**, *109*, 10570.
(29) Brandt, P.; Norrby, T.; Akermark, B. *Inorg. Chem.* **1998**, *37*, 4120.
(30) Salzmann, R.; Ziegler, C. J.; Godbout, N.; Mcmahon, M. T.; Suslick, K. S.; Oldfield, E. *J. Am. Chem. Soc.* **1998**, *120*, 11323.
(31) Karlsson, A.; Broo, A.; Ahlberg, P. *Can. J. Chem.* **1999**, *77*, 628.
(32) Hermann, K.; Witko, M. *J. Mol. Struct. (THEOCHEM)* **1999**, *458*, 81.
(33) Citra, A.; Andrews, L. *J. Phys. Chem. A* **2000**, *104*, 6.
(34) Tobisch, S.; Nowak, T.; Bögel, H. *J. Organomet. Chem.* **2001**, *619*, 24.
(35) Zheng, K. C.; Kuang, D. B.; Wang, J. P.; Shen, Y. *Acta Phys.-Chim. Sin.* (in Chinese) **2000**, *16*, 608.
(36) Zheng, K. C.; Kuang, D. B.; Wang, J. P.; Shen, Y. *Chin. J. Chem. Phys.* **2000**, *13*, 551.
(37) Zheng, K. C.; Kuang, D. B.; Shen, Y.; Wang, J. P. *Acta Phys.-Chim. Sin.* (in Chinese) **2001**, *17*, 43.
(38) Zheng, K. C.; Wang, J. P.; Shen, Y.; Kuang, D. B.; Yun, F. C. *Acta Chim. Sin. (Huaxue Xuebao*, in Chinese) **2001**, *59*, 1283.

(39) Zheng, K. C.; Wang, J. P.; Shen, Y.; Kuang, D. B.; Yun, F. C. *J. Phys. Chem. A* **2001**, *105*, 7248.

(40) Zheng, K. C.; Wang, J. P.; Liu, X. W.; Shen, Y.; Yun, F. C. *J. Mol. Struct. (THEOCHEM)*, in press.

(41) Schaftenaar, G. *Molden v3.6*; University of Nijmegen, Nijmegen, The Netherlands, 1999.

(42) Foresman, J. B.; Frisch, Æ. *Exploring Chemistry with Electronic Structure Methods*, 2nd ed.; Gaussian Inc.: Pittsburgh, PA, 1996.

(43) Carpenter, J. E.; Weinhold, F. *J. Mol. Struct. (THEOCHEM)* **1988**, *169*, 41.

(44) Pople, J. A.; Gordon, M. *J. Am. Chem. Soc.* **196**7, *89*, 4253.

(45) Fliszar, S. *J. Am. Chem. Soc.* **1972**, *94*, 1068.

(46) Chen, Z. X. *J. Mol. Sci.* **1983**, *1*, 65.

(47) Zheng, K. C.; He, F.; Xu, Z. T.; Yun, F. C. *Acta Phys.-Chim. Sin.* (in Chinese) **1999**, *15*, 698.

(48) Zheng, K. C.; Kuang, D. B.; Yun, F. C.; He, F. *Acta Phys.-Chim. Sin.* (in Chinese) **2000**, *16*, 133.

(49) Gao, X. H.; Chen, T. L. *Chin. Sci. Bull.* (in Chinese) **1980**, *25*, 254.

(50) Hitchcock, P. B.; Seddon, K. R.; Turp, J. E.; Yousif, Y. Z.; Zora, J. A. *J. Chem. Soc., Dalton Trans.* **1988**, 1837.

(51) Belser, P.; Zelewsky, A. V.; Zehnder, M. *Inorg. Chem.* **1981**, *20*, 3098.

(52) Rillema, D. P.; Jones, D. S.; Levy, H. A. *J. C. S. Chem. Comm.* **1979**, 849.

(53) Fleming, I. *Frontier Orbital and Organic Chemical Reaction*; Wiley: New York, 1976.

(54) Gorling, A. *Phys. Rev.* **1996**, *54*, 3912.

(55) Rutherford, T. J.; Pellegrini, P. A.; Aldrich-Wright, J.; Junk, P. C.; Keene, F. R. *Eur. J. Inorg. Chem.* **1998**, 1677.

(56) Juris, A.; Belser, P.; Barigelletti, F.; Zelewsky, A. V.; Balzani, V. *Inorg. Chem.* **1986**, *25*, 256.

(57) Graham Solomons, T. W. *Organic Chemistry*, 6th ed.; Wiley: New York, 1996; p 680.